

Observation of Layered Structures and Laue Patterns in Coulomb Glasses

Shuji Ogata and Setsuo Ichimaru

Department of Physics, University of Tokyo, Bunkyo-ku, Tokyo 113, Japan

(Received 5 October 1988)

We report the first observation of layered structures in the computer-simulated Coulomb glasses produced by rapid quenching of one-component plasmas in the absence of an external force field. Degrees of polycrystalline nucleation and the nature of local order developed in the glasses are elucidated through analyses of the intralayer and interlayer particle correlations and by means of the Laue patterns formed by scattering of plane waves. Stages of evolution for the glass transition in Coulombic systems are conjectured.

PACS numbers: 64.60.Cn, 61.20.Ja, 61.50.Ks, 64.70.Pf

Recent experimental¹ and computer-simulation^{2,3} studies on the strongly coupled systems (i.e., $\Gamma \gg 1$) of charged particles in an external force field have revealed that the internal order develops through a formation of layered structures in the direction of the external field. For a classical one-component plasma (OCP) with electric charge Ze , number density n , and temperature T , the Coulomb-coupling constant⁴ is $\Gamma = (Ze)^2/akT$, where $a = (4\pi n/3)^{-1/3}$ is the ion-sphere radius; hereafter lengths will be measured in units of a , unless specified otherwise.

In this Letter, we wish to report the first observation of analogous layered structures in Coulomb glasses *without* an external force field, which are produced by rapid quenching of OCP's in Monte Carlo (MC) simulations. We investigate the degrees of polycrystalline nucleation and the nature of local bond-orientational order developed in the glasses, and analyze the intralayer and interlayer particle correlations by means of the Laue patterns formed by scattering of plane waves.

Dynamic evolution and formation of Coulomb glasses by the MC method have been described elsewhere.⁵ Four distinct runs of the MC simulations with 432 particles were performed starting with the equilibrated fluid state at $\Gamma = 160$: (A) an application of a sudden quench to $\Gamma = 400$ at $c = 0$, (B) an application of a gradual quench stepwise with $\Delta\Gamma = 10$ from $\Gamma = 160$ at $c = 0$ to $\Gamma = 400$ at $c = 23$, (C) a sudden quench to $\Gamma = 300$ at $c = 0$, and (D) a sudden quench to $\Gamma = 200$ at $c = 0$. Here c denotes the sequential number of MC configurations measured in units of a million configurations; the sequential number corresponds to the MC time^{5,6} via $\omega_p t = 2.7 \times 10^2 c$, with ω_p referring to the plasma frequency.

Evolution of the internal energy, correlation functions, and bond-orientational order was monitored up to $c = 80$ for (A)-(C) and up to $c = 30$ for (D); we thereby confirmed establishment of metastable final states.⁵ While the quench (D) resulted in a supercooled *fluid* state, we found that the metastable states in the quenches (A)-(C) formed *Coulomb glasses*, which were

characterized by random polycrystalline structures with long-ranged bond-orientational order; the particles were virtually locked around their equilibrium positions.^{5,7} The polycrystalline structures and the degrees of nucleation differed delicately from each other among the glasses (A)-(C); here these features will be clarified further through investigation of the layered structures and the Laue patterns.

In the metastable states of the quenches (A)-(C), we consider configurations of MC particles contained in the sphere with a radius $L/2$ inscribed to the cube L^3 of the MC cell; the Cartesian axes (x, y, z) are set along the MC cell. The sphere as a whole is then rotated by an angle ζ around the y axis and by an angle η around the z axis; the resulting configuration of the particles is projected onto a y - z plane. For each of the metastable glasses, we construct such projection maps of particle configurations for 21×21 different combinations of ζ and η between 0 and $\pi/2$. In Fig. 1, we exhibit sample maps [(A) $\zeta = \pi/20$, $\eta = \pi/2$; (B) $\zeta = 3\pi/20$, $\eta = 0$; (C) $\zeta = 17\pi/40$, $\eta = \pi/40$] displaying formation of a layered structure in the particle configurations in the quenches (A)-(C). (Although not shown here, many of the maps are of disordered configurations.) Those different values of ζ and η involved in the observation of the ordered configurations imply that the effects of the periodic boundary conditions are *not* significant in the formation of the layered structures. This statement will be further substantiated later through observation of a simulation run with a larger ($N = 1458$) system.

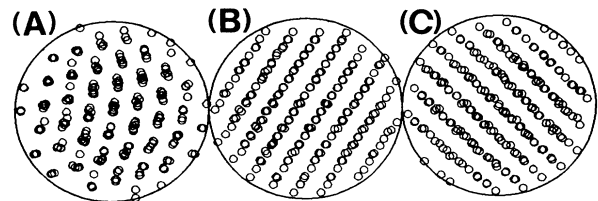


FIG. 1. Projection maps of particle configurations for the glasses (A)-(C).

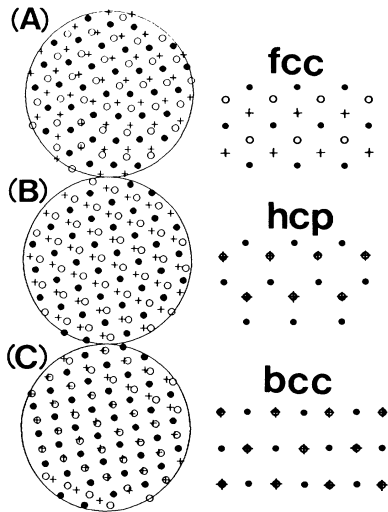


FIG. 2. Normal projections of most closely packed layers: open circles, upper layer; closed circles, middle layer; crosses, lower layer.

We have thus confirmed the existence of layered structures in the Coulomb glasses produced with the quenches (A)–(C). The observed interlayer separations are 1.424 ± 0.006 for (A), 1.468 ± 0.002 for (B), and 1.425 ± 0.007 for (C). These are to be compared with the separations between the most closely packed layers (cf. Fig. 2) in the crystals; they are 1.477 for the fcc and hcp lattices, and 1.436 for the bcc lattice. The interlayer separation for (B) thus falls between those for the fcc-hcp and bcc lattices, and has the smallest value of uncertainty (meaning layers of least warping). These results corroborate precisely the earlier findings⁵ that the Coulomb glass with the quench, (B), has developed to an advanced state of polycrystalline nucleation predominantly with local fcc-hcp configurations, while the glasses (A) and (C) are in states with lesser degrees of nucleation.

To study the nature of interlayer correlations, we identify the particles in the three central layers and project their positions normally onto a plane. In Fig. 2, such projections are shown for the quenches (A)–(C), where the open circles denote projections of the particles on the upper layer; the closed circles, those on the middle layer; and the crosses, those on the lower layer. For comparison, analogous projections are shown in Fig. 2 for the most closely packed layers in the fcc, hcp, and bcc crystals. Here again we observe an advanced degree of nucleation in the quenched state (B) dominated by fcc-hcp configurations.

Intralayer correlations are investigated in terms of the bond-angle distributions $P(\theta)$ (Fig. 3) and the two-dimensional radial distribution functions $g(r)$ (Fig. 4). We define “bonds” as those lines connecting two adjacent particles located within $r < 2.5$ on a layer, “bond angle” as the angle between a pair of such bonds origi-

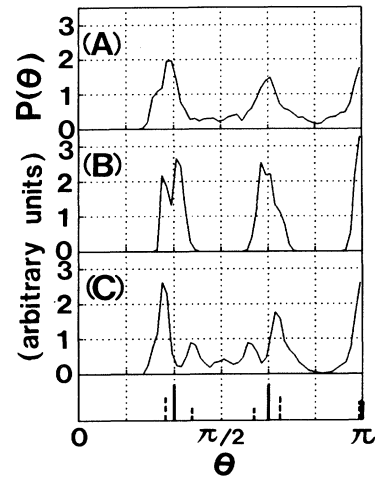


FIG. 3. Bond-angle distribution functions between intralayer particles in the glasses (A)–(C). In the bottom of the figure, the solid lines indicate the bond angles for the fcc-hcp (hexagonal) lattices; the dashed lines, those for the bcc lattices.

nating from a particle, and “coordination number” (CN) as the total number of bonds originating from a given particle.

In Fig. 3, we plot the bond-angle distribution functions between intralayer particles in the quenched states (A)–(C), and compare them with analogous quantities for the fcc-hcp (i.e., hexagonal) and bcc lattices. In the state (B), $P(\theta) = 0$ observed at $\theta \sim \pi/2$ and $5\pi/6$ implies an advanced degree of nucleation, while splitting of the peaks at $\theta \sim \pi/3$ and $2\pi/3$ indicates disordering effects on the local hexagonal configurations.

In Fig. 4, we plot the two-dimensional radial distribution functions between intralayer particles and compare them with the peak positions for the fcc-hcp and bcc lat-

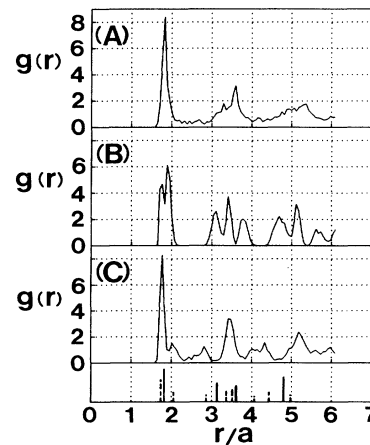


FIG. 4. Two-dimensional radial distribution functions between intralayer particles in the glasses (A)–(C). The bottom of the figure shows the peak positions for the fcc-hcp (solid lines) and bcc (dashed lines) lattices.

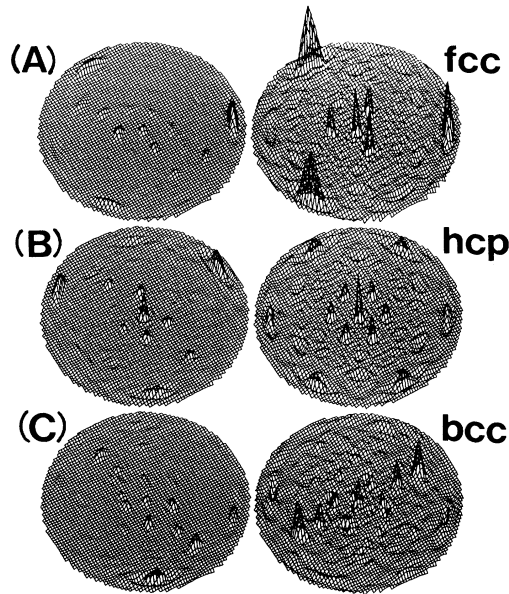


FIG. 5. Laue patterns for the glasses (A)–(C) and for the fcc, hcp, and bcc lattices of 432 particles. The polar coordinates consist of $0 \leq (\pi - \chi)/2 \leq 0.45\pi$ and $0 \leq \phi \leq 2\pi$; the origin corresponds to $\chi = \pi$.

tices. As seen in the figure, all the particles in the state (B) have CN=6, implying little distortion in the local hexagonal configurations. In the states (A) and (C), however, distortion in the hexagonal configurations is substantial, since 89% and 90%, respectively, of the particles have CN=6, while 5% and 8% have CN=5, and 6% and 2% have CN=7.

Finally, we investigate the combined effects between the intralayer and interlayer correlations by a scattering method. To do so, we inject plane waves with wave vector \mathbf{k}_1 to the glasses (A)–(C) in the direction normal to the layered structures, and measure the strength of scattered waves \mathbf{k}_2 in the direction specified by (χ, ϕ) , where χ is the scattering angle between \mathbf{k}_1 and \mathbf{k}_2 and ϕ is the azimuthal angle around \mathbf{k}_1 . The cross section for coherent scattering is proportional to the structure factor,⁸

$$S(\mathbf{k}) = \left\langle \left| \sum_j \exp(i\mathbf{k} \cdot \mathbf{r}_j) \right|^2 \right\rangle \quad (\mathbf{k} = \mathbf{k}_2 - \mathbf{k}_1).$$

We assume that the incident wave numbers have a distribution proportional to $\exp[-(k_1 - k_0)^2/\kappa^2]$ with $k_0 = 2\pi$ and $\kappa = 0.24$. The scattering experiment is thus capable of detecting the coherence in the phases $4\pi \sin(\chi/2) \mathbf{k} \cdot \mathbf{r}_j/k$ over those particles \mathbf{r}_j contained in a slab of width $4.2/\sin(\chi/2)$ in the direction of \mathbf{k} .

Figure 5 displays the Laue patterns thus obtained for the glass states (A)–(C), and compares them with those of the fcc, hcp, and bcc lattices. We observe the existence of local hexagonal order in (B) and to a lesser extent in (A); a slight involvement of local bcc

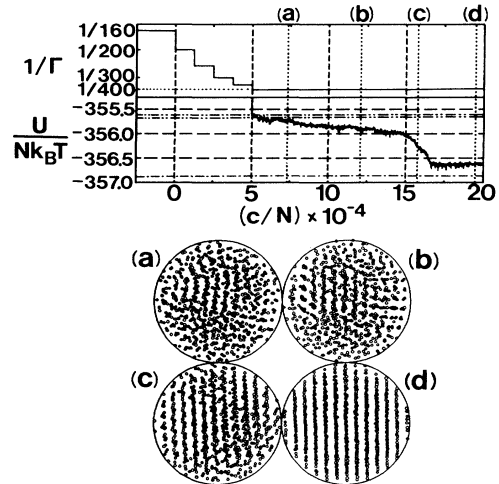


FIG. 6. Upper: Variation of $1/\Gamma$ in the MC simulation run with $N=1458$. Middle: Evolution of the normalized excess internal energy (see Ref. 5) with specification of the stages (a)–(d). Lower: Projection maps of particle configurations at $\zeta=11\pi/40$ and $\eta=2\pi/5$ in the stages (a)–(d). In this figure c means the number of MC configurations (not in units of 10^6).

configurations is likewise detected for all the cases of (A)–(C). The Laue pattern obtained for the supercooled fluid state with the quench, (D) (not shown here), on the other hand, exhibits no coherent structures, and hence implies absence of locally ordered configurations. (We have quantified the Laue-pattern analyses by calculating Fourier components of the intensity distributions with respect to ϕ ; the results have sustained the aforementioned observations.)

In conclusion, in light of the analyses described above, we may conjecture the following stages of evolution for the glass transition in Coulombic systems: In a supercooled OCP without an external field, layered structures (i.e., an one-dimensional order) develop first in an arbitrary direction. Intralayer (i.e., two-dimensional) ordering then follows, which would favor the formation of the fcc-hcp (i.e., hexagonal) local clusters. Since the bcc lattice has a Madelung energy slightly lower than the fcc or hcp lattice in Coulombic systems,⁵ however, a possibility of nucleation remains for bcc clusters. A Coulomb glass is affected by those combined effects of ordering; hence the resulting state has a complex polycrystalline structure.

After completing the bulk of the work reported above, we have performed a MC simulation run with a larger system ($N=1458$) over 3×10^8 configurations. Although the detailed results are to be reported in a later publication,⁹ we show Fig. 6 here which clearly displays how the layered structures develop *internally* as the equilibration proceeds. Quenching processes and stages (a)–(d) are defined in the upper part of the figure; the projection maps (a)–(d) in the lower part of the figure are taken at the same rotation angles: $\zeta=11\pi/40$ and

$\eta=2\pi/5$. The layered structures observed in the final stage (d) are much more regular in this larger system than those in Fig. 1, and we can show⁹ that the stage (d) in fact corresponds to a bcc crystalline state. Figures 1 and 6 thus demonstrate that the layered structures in the final states are independent of the initial conditions and are not the products of the periodic boundary conditions in the MC simulations.

This work was supported in part through Grants-in-Aid for Scientific Research provided by the Ministry of Education, Science and Culture of Japan.

¹S. L. Gilbert, J. J. Bollinger, and D. J. Wineland, Phys.

Rev. Lett. **60**, 2022 (1988)

²A. Rahman and J. P. Schiffer, Phys. Rev. Lett. **57**, 1133 (1986); J. P. Schiffer, Phys. Rev. Lett. **61**, 1843 (1988).

³D. H. E. Dubin and T. M. O'Neil, Phys. Rev. Lett. **60**, 511 (1988).

⁴For a review, see, e.g., S. Ichimaru, H. Iyetomi, and S. Tanaka, Phys. Rep. **149**, 91 (1987).

⁵S. Ogata and S. Ichimaru, Phys. Rev. A **39**, 1333 (1989).

⁶S. Ogata and S. Ichimaru, Phys. Rev. A **38**, 1457 (1988); the scheme A in this reference has been used for the displacements in the present MC simulations.

⁷See Ref. 5 for averaging on particle positions.

⁸See, e.g., D. Pines, *Elementary Excitations in Solids* (Benjamin, New York, 1963), Sec. 4-4.

⁹S. Ogata and S. Ichimaru, J. Phys. Soc. Jpn. **58**, 356 (1989); (unpublished).